

# Rheology of High-Capillary Number Flow in Porous Media

Santanu Sinha

*Beijing Computational Science Research Center, 10 East Xibeiwang Road, Haidian District, Beijing 100193, China.*

Magnus Aa. Gjennestad,, Morten Vassvik,, Mathias Winkler, and Alex Hansen

*PoreLab, Department of Physics, Norwegian University of Science and Technology, NO-7491 Trondheim, Norway.*

Eirik G. Flekkøy

*PoreLab, Department of Physics, University of Oslo,  
P.O. Box 1048 Blindern, NO-0316 Oslo, Norway*

(Dated: September 19, 2018)

Immiscible fluids flowing at high capillary numbers in porous media may be characterized by an effective viscosity. We demonstrate that the effective viscosity is well described by the Lichtenecker-Rother equation. The exponent  $\alpha$  in this equation takes either the value 1 or 0.6 in two- and 0.5 in three-dimensional systems depending on the pore geometry. Our arguments are based on analytical and numerical methods.

PACS numbers:

The hydrodynamics of real things very often happens at small scale, i.e. in a porous medium [1]. This is the case in a wide variety of biological, geological and technological systems where there are normally several immiscible fluids present. The challenge of describing such systems in a unified way, however, is largely unsolved. An important reason for this is the lack of a length scale above which the system may be averaged as if it were homogeneous. Such a length scale gives rise to the so-called representative elementary volume (REV) which is the conceptual basis for conventional theories that seek to up-scale the description of flow in porous media. However, since the fluid structures in question are often fractal, the REV average of intensive quantities, such as saturations, will depend on the size of the REV.

An important and rather general exception where this is not a problem, is the case of steady states [2, 3]. Steady states are characterized by potentially strong fluctuations at the pore scale, but with steady averages at the REV scale. As such they differ fundamentally from stationary states that are static at the pore scale as well. Steady states have much in common with ensembles in equilibrium statistical mechanics. These states are implicitly assumed in conventional descriptions of porous media flows that take the existence of an REV for granted.

When the flows in question contain immiscible phases that are strongly forced in the sense that viscous forces dominate capillary forces, the description of the steady state simplifies to the description of a single fluid. This is the subject of the present letter, and we show how the emergent description is manifestly incompatible with the conventional theories that have been in use for more than 80 years, most notably perhaps by the petroleum industry.

The first and still leading theory describing immiscible two-phase flow in porous media is that of Wyckoff and Botset [4] who based their theory of relative permeability on the idea that when the porous medium is seen

from the viewpoint of one of the fluids, the pore volume accessible to this fluid would be the pore volume of the porous medium minus the pore volume occupied by the other fluid. This reduces the effective permeability seen by either fluid and the relative reduction factor is the relative permeability. In order to account for the surface tension between the immiscible fluids in the pores, the concept of capillary pressure was introduced by Leverett [5]. The central equations in relative permeability theory are the generalized Darcy equations

$$\vec{v}_j = -\frac{K}{\mu_j} k_{r,j}(S_j) \vec{\nabla} P_j, \quad (1)$$

where the subscript  $j$  either refers to the wetting fluid ( $j = w$ ) or the non-wetting fluid ( $j = n$ ).  $\vec{v}_w$  and  $\vec{v}_n$  are superficial velocities of the wetting and non-wetting fluids, respectively. They are defined as the volumetric flow rates of each fluid entering a REV divided by the area of entry.  $K$  is the permeability of the porous medium,  $\mu_w$  and  $\mu_n$  are the wetting and non-wetting viscosities.  $k_{r,w}(S_w)$  and  $k_{r,n}(S_w)$  are the relative permeabilities of the wetting and non-wetting fluids and they are both functions of the wetting saturation  $S_w$  only. The corresponding non-wetting saturation is  $S_n$  and we have that  $S_w + S_n = 1$ . The wetting and non-wetting pressure fields  $P_w$  and  $P_n$  are related through the capillary pressure function  $P_c(S_w) = P_n - P_w$ . We may define a total superficial velocity  $\vec{v}$

$$\vec{v} = \vec{v}_w + \vec{v}_n. \quad (2)$$

This is the volumetric flow rate of all fluids entering the REV divided by the area of entry.

Let us now suppose that the flow rates are so large that the capillary pressure may be ignored. Hence, we have  $P_n = P_w = P$  and we may combine the relative

permeability equations (1) with equation (2) to find

$$\vec{v} = -K \left[ \frac{k_{r,w}(S_w)}{\mu_w} + \frac{k_{r,n}(S_n)}{\mu_n} \right] \vec{\nabla} P = -\frac{K}{\mu_{\text{eff}}(S_w)} \vec{\nabla} P, \quad (3)$$

where we have defined an *effective viscosity*  $\mu_{\text{eff}}$

$$\frac{1}{\mu_{\text{eff}}(S_w)} = \frac{k_{r,w}(S_w)}{\mu_w} + \frac{k_{r,n}(S_n)}{\mu_n}. \quad (4)$$

There have been many suggestions as to what functional form the relative permeabilities  $k_{r,w}(S_w)$  and  $k_{r,n}(S_n)$  take. The most common choice is to use the Brooks–Corey relative permeabilities assuming  $k_{r,w}(S_w) = k_{r,w}^0 S_w^{n_w}$  and  $k_{r,n}(S_n) = S_n^{n_n}$  where  $0 \leq k_{r,w}^0 \leq 1$  and the two Corey exponents  $n_w$  and  $n_n$  are typically in the range 2 to 6 [6, 7].

Equation (4) is problematic. When  $\mu_w = \mu_n$ , a dependency of  $\mu_{\text{eff}}$  on the saturation is predicted when  $n_w$  and/or  $n_n$  are larger than 1 when using the Brooks–Corey relative permeabilities. Other functional forms for the relative permeabilities give similar dependencies. Clearly, such behavior is not physical.

McAdams et al. [8] proposed an effective viscosity for two-phase flow by assuming a saturation-weighted *harmonic* average

$$\frac{1}{\mu_{\text{eff}}} = \frac{S_w}{\mu_w} + \frac{S_n}{\mu_n}. \quad (5)$$

On the other hand, Cicchitti et al. [9] proposed an effective viscosity based on the saturation-weighted *arithmetic* average

$$\mu_{\text{eff}} = \mu_w S_w + \mu_n S_n. \quad (6)$$

Both of these expressions become saturation-independent when  $\mu_w = \mu_n$  as they should. There are several other proposals for the functional form of the effective viscosity  $\mu_{\text{eff}}$  in the literature [10].

A one-dimensional porous medium, i.e. a capillary tube where the two fluids move as bubbles in series [11] constitutes a series coupling and the arithmetic average (6) is the appropriate one. On the other hand, if the capillary tubes form a parallel bundle each filled with either the wetting or the non-wetting fluid, we have a parallel coupled system and equation (5) is appropriate. Suppose now that each capillary  $i$  in the bundle is filled with a bubble train with a corresponding wetting saturation  $S_{w,i}$ . The probability distribution for finding a capillary having this saturation,  $S_{w,i}$ , is  $p(S_{w,i})$ . We have that

$$S_w = \int_0^1 dS p(S) S. \quad (7)$$

The effective viscosity for the capillary bundle is then given by

$$\frac{1}{\mu_{\text{eff}}} = \int_0^1 \frac{p(S) dS}{\mu_w S + \mu_n (1-S)}. \quad (8)$$

As a model for the distribution  $p(S_{w,i})$ , we may take a gaussian with a narrow width  $\sigma$  centered around  $S_w$ :  $p(S_{w,i}) = \exp[-(S_{w,i} - S_w)^2 / 2\sigma^2] / \sqrt{2\pi\sigma^2}$ . Using a saddle point approximation, we find to order  $\sigma^2$  that

$$\mu_{\text{eff}} = \mu_w S_w + \mu_n S_n - \frac{(\mu_n - \mu_w)^2}{\mu_w S_w + \mu_n S_n} \sigma^2. \quad (9)$$

We now consider a wide distribution of saturations in each capillary:  $p(S_{w,i})$  is uniform rather than gaussian. We set the average wetting saturation to the value  $S_w = 1/2$ , finding

$$\mu_{\text{eff}} = \left| \frac{\mu_w - \mu_n}{\ln\left(\frac{\mu_w}{\mu_n}\right)} \right|. \quad (10)$$

The functional form of the latter equation is very different from the gaussian, equation (9).

The extreme case when the capillaries are either filled completely by the wetting or the non-wetting fluid corresponds to  $p(S_{w,i}) = S_w \delta(S_{w,i} - 1) + S_n \delta(S_{w,i})$  giving, as already pointed out, an effective viscosity according to equation (5). We may, however, study this either-or situation in a more complex network, namely a square lattice. We assume that the wetting saturation is set to  $S_w = 1/2$ , which defines the percolation threshold for bond percolation and that the links are randomly filled with either fluid. By analogy with the percolation problem we may use Straley's exact result [12] leading to an effective viscosity given by

$$\mu_{\text{eff}} = \sqrt{\mu_w \mu_n}. \quad (11)$$

We may calculate the effective viscosity of a regular lattice by using Kirkpatrick's mean field theory [17], first introduced as a tool to calculate the conductivity of a percolating set of conductors with random values. In that case conductances are fixed in time and space, giving rise to a problem different from ours where the fluids are free to distribute themselves in a non-trivial way and create flow paths where conductances vary dynamically.

The mobility between nodes  $i$  and  $j$  is  $K_{ij}/\mu_{ij}$  where  $K_{ij}$  is the permeability and  $\mu_{ij} = \mu_w S_{w,ij} + \mu_n S_{n,ij}$  is the effective viscosity of the link and the saturations take on their local values. The form of  $\mu_{ij}$  reflects the fact that the fluids contained in the link are connected in series.

Kirkpatrick's theory is based on the notion that the network of mobilities  $K_{ij}/\mu_{ij}$  may be replaced by a network of links with a single mobility  $K/\mu_{\text{eff}}$  but with the same total network mobility. The value of  $K/\mu_{\text{eff}}$  is given by the formula [17]

$$\left\langle \frac{\frac{K}{\mu_{\text{eff}}} - \frac{K_{ij}}{\mu_{ij}}}{\frac{K_{ij}}{\mu_{ij}} + \left[\left(\frac{z}{2}\right) - 1\right] \frac{K}{\mu_{\text{eff}}}} \right\rangle = 0, \quad (12)$$

where  $z$  is the coordination number of the lattice, and the ensemble average  $\langle \dots \rangle = \int_0^\infty dK_{ij} P(K_{ij}) \int_0^1 dS_{w,ij} p(S_{w,ij}) \dots$ ,  $P(K_{ij})$  being

the permeability distribution and  $p(S_{w,ij})$  is the wetting saturation distribution fulfilling (7). We assume a square lattice so that  $z = 4$ .

By assuming that the saturation distribution is a narrowly peaked gaussian with width  $\sigma$ , we may again use the saddle point approximation giving

$$\mu_{\text{eff}} = \mu_w S_w + \mu_n S_n + \mathcal{O}(|\mu_n - \mu_w| \sigma^2). \quad (13)$$

This result is similar to that found for the parallel capillary bundle, see equation (9).

From these model systems giving rise to equations (9), (10), (11) and (13) we see that it is far from obvious what the effective viscosity  $\mu_{\text{eff}}$  should be. Does it depend on the details of the porous medium or can one find a general form? We may generalize equations (5) and (6) by writing them in the form

$$\mu_{\text{eff}}^\alpha = \mu_w^\alpha S_w + \mu_n^\alpha S_n, \quad (14)$$

where  $\alpha = -1$  for parallel coupling — equation (5) — and  $\alpha = +1$  for series coupling — equation (6). The effective viscosity in (11) corresponds to  $\alpha = 0$ , whereas equations (9) and (13) suggest  $\alpha = 1$ . Only the effective viscosity in equation (10) does not fit this form. Equation (14) has been used for estimating the effective electrical permittivity of heterogeneous conductors and in connection with permeability homogenization in porous media. It is known as the Lichtenecker–Rother equation [13–16].

We now proceed with numerical methods to test whether the proposed form (14) adequately describes the effective viscosity. We use two approaches; dynamic pore-network modeling and Lattice Boltzmann modeling. In the dynamic pore-network modeling [18], the porous medium is represented by a network of links, connected at nodes, which transport two immiscible fluids separated by interfaces. We implement periodic boundary conditions, which keeps the saturation constant with time. The flow rate of the fluids inside a link between two neighboring nodes  $i$  and  $j$  obeys the constitutive equation

$$q_{ij} = -\frac{g_{ij}}{l_{ij}} [p_j - p_i], \quad (15)$$

where  $p_i$  and  $p_j$  are the local pressure drops at the nodes. Here  $l_{ij}$  and  $g_{ij}$  are respectively the length and the mobility of the link. There is no contribution to the pressure from interfaces in the link as the surface tension has been set to zero. The mobility  $g_{ij}$  is inversely proportional to the link viscosity given by  $\mu_{ij} = \mu_w S_{w,ij} + \mu_n S_{n,ij}$ . Simulations are performed with a constant global pressure drop  $\Delta P$  across the network. We determine the local pressures  $p_i$  by solving the Kirchhoff equations using the conjugate gradient algorithm. Local flow rates  $q_{ij}$  through each link are then calculated using equation (15) and the interfaces are advanced with appropriate time steps.

A crucial point is the distribution of the two fluids after they mix at the nodes and enter the next links. Whether the system allows high or low fragmentation of

the fluids, will depend on the geometry of the porous media and the nature of the pore space [19, 20]. This will have impact on the size of the bubbles and the number of interfaces inside a link. Note that small bubbles of either fluid may not necessarily imply a large number of interfaces or vice-versa. We therefore implemented two different algorithms for the interface dynamics. In the *bubble-controlled* algorithm, we limit the minimum size of a bubble before entering in a link and in the *interface-controlled* algorithm we limit the maximum number of interfaces that can exist in a link. We then considered two different possibilities for each algorithm, for the bubble-controlled case, (A) bubbles with lengths at least equal to the respective pore radii, i.e  $b_{\text{min}} \geq r_{ij}$  and (B) bubble sizes can be much smaller,  $b_{\text{min}} \geq 0.02r_{ij}$ . For the interface-controlled algorithm, we studied two cases, (C) one with maximum 2 and (D) another with maximum 4 interfaces per link. For a detailed description of the two algorithms for the interface dynamics, we refer to the supplementary material.

We consider both two-dimensional (2D) and three-dimensional (3D) networks. For 2D, we used square lattices of  $64 \times 64$  links and honeycomb lattices of size  $64 \times 40$  links where all the links have the same length  $l$ , and their radii  $r_{ij}$  are uniformly distributed in the interval  $0.1 l < r < 0.4 l$ . The square network was oriented at  $45^\circ$  with respect to the overall flow direction. For A and B, results of honeycomb lattices will be presented, and for C and D, we will present the results of square lattices. For 3D, two reconstructed pore networks extracted from the real samples were used; one is a Berea sandstone containing 1163 nodes and 2274 links, and the another is a sand pack with 767 nodes and 1054 links [21]. The links for the 2D networks have circular cross section which corresponds  $g_{ij} = \pi r_{ij}^4 / (8\mu_{ij})$ . For the 3D networks, the links have triangular cross section and the mobility terms are calculated considering their shape factors [21–23].

Effective viscosities  $\mu_{\text{eff}}$  measured in the steady state for models A and C (large bubbles or few interfaces) are plotted in figure 1. Results are then compared with  $(\mu_{\text{eff}}/\mu_w)^\alpha = S_w + M^\alpha S_n$ , see equation (14), where  $M = \mu_n/\mu_w$ , and found consistent with  $\alpha = 0.6$  for 2D and with  $\alpha = 0.5$  for 3D. In figure 2, we show  $\mu_{\text{eff}}/\mu_w$  for models B and D (small bubbles or many interfaces) and the results show  $\alpha = 1$  for both 2D and 3D. We show typical configurations for models C and D in the supplementary material.

In summary we find for network models B and D, where there are the minimum bubble size is 0.02 times the link radius (B), or up to four interfaces (D) a result which is consistent with the Kirkpatrick mean field theory,  $\alpha = 1$ . For the models with minimum bubble sizes being larger than the link radii (A) or with a maximum number of interfaces equal to 2 (C), we find a much smaller  $\alpha = 0.6$  in 2D and 0.5 in 3D (model C). Using the bubble-controlled model, we have varied the minimum bubble size over the range  $0.02r_{ij}$  to  $0.5r_{ij}$  finding  $\alpha$  decreasing gradually from 1 to 0.6. Taking into ac-

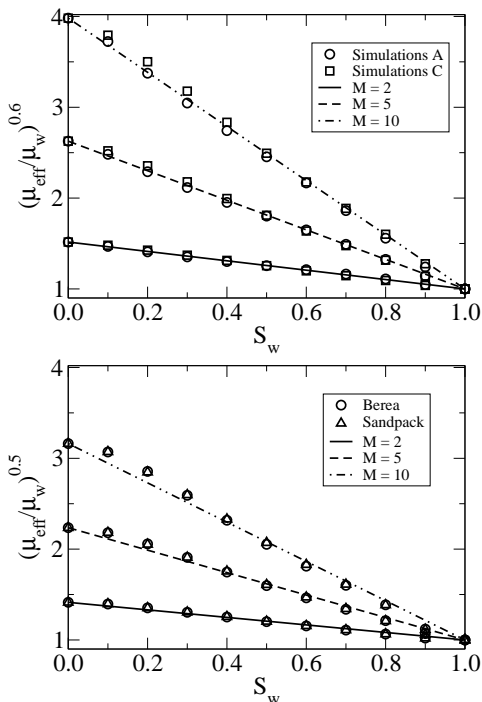


FIG. 1: Values of  $(\mu_{\text{eff}}/\mu_w)^\alpha$  obtained from the network simulations for the cases A and C, the large bubbles and few interfaces respectively, plotted with different symbols as a function of the wetting saturations ( $S_w$ ). Results are compared with  $S_w + M^\alpha S_n$ , equation (14), plotted with straight lines, and found consistent with  $\alpha = 0.6$  for two-dimensions and  $\alpha = 0.5$  for three dimensions.

count that  $r_{ij} \leq 0.4 l$ , where  $l$  is the link length, this shift of  $\alpha$  from 1 to 0.6 occurs over the narrow range from  $0.008 l$  to  $0.2 l$ , indicating that we are dealing with a crossover.

Figure 3 shows the wetting volumetric fractional flow rate  $F_w$  as a function of the wetting saturation  $S_w$  for a maximum of 2 (C) or 4 interfaces (D). The data for model D gives  $F_w = S_w$  both in 2D and 3D. This indicates that when the maximum number of interfaces in the links is higher, the fluids mix at the link level and they act as if there is no viscosity contrast between them. On the other hand, the maximum number of interfaces is small, the viscosity contrast it felt and the least viscous fluids flow the fastest.

Next, we turn to a lattice Boltzmann model which has no explicit parameters for the bubble size or the number of interfaces and permits arbitrary shapes of the fluid domains within the link. We base it on the original triangular lattice and the interaction rules first introduced by Gunstensen *et al.* [24]. We implemented the model on a  $128 \times 128$  biperiodic lattice. The size is rather small, but suffices to simulate a representative  $4 \times 4$  pipe-network, and is chosen in part to keep the Reynolds number around 1 or smaller. The capillary number  $Ca$  was larger than 9. The pressure gradient was implemented as a constant body force in the diagonal direction.

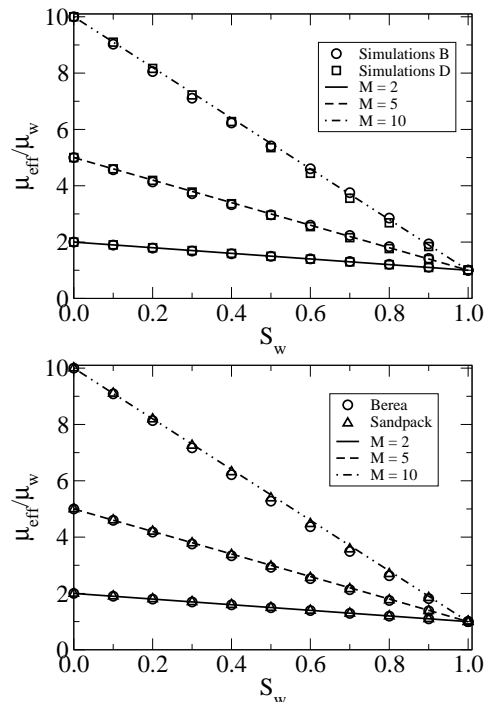


FIG. 2: Plot of  $(\mu_{\text{eff}}/\mu_w)^\alpha$  obtained from the network simulations (symbols) for the cases B and D, small bubbles and many interfaces respectively, as a function of  $S_w$  and compared with  $S_w + M^\alpha S_n$  (straight lines). Here the numerical results are consistent with  $\alpha = 1$  for both 2D and 3D.

The simulations with a given pressure gradient and measured flow rate were performed. In figure 4 the effective viscosity is plotted as a function of  $S_w$ . The spread in the measurements at constant  $S_w$  result from the variability in the flow velocity corresponding to fluctuations in the local viscosity values. The straight lines are consistent with  $\alpha = 1$  in equation (14). This may be the result of the large length to width ratio used for the links. The fluids were found to organize in a way that combines both fluid elements in parallel and in series, i.e. there are both string- and plug-like structures, see the supplementary material.

We have studied the effective viscosity of immiscible two-fluid flow in porous media in the high capillary number limit where the capillary forces may be ignored compared to the viscous forces. We find that the Lichtenecker–Rother equation (14) describes the effective viscosity well. The exponent depends on the fluid configuration, i.e. the number of bubbles/interfaces in the pores. For small bubbles or many interfaces in the pores, as with the Boltzmann model, we find  $\alpha = 1$ , whereas when the bubbles are larger or the interfaces fewer in the pores, we find  $\alpha = 0.6$  in 2D (square and hexagonal lattices) and  $\alpha = 0.5$  in 3D for networks reconstructed from Berea sandstone and sand packs. The exponent  $\alpha$  depends on the pore geometry.

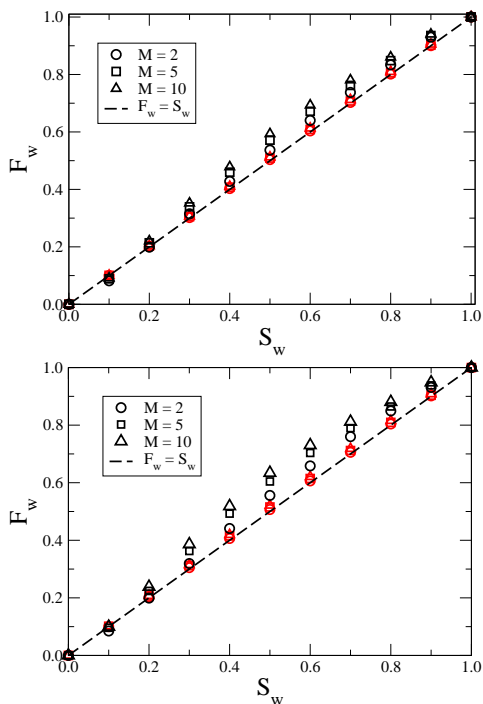


FIG. 3: Comparison of the wetting fractional flow ( $F_w$ ) for 2D (left) and 3D (right) networks. Results from simulations with a maximum of 2 interfaces, case C (black symbols), and simulations allowing up to 4 interfaces, case D (red symbols). The straight line represents  $F_w = S_w$ , if both the fluids flow with same velocity.

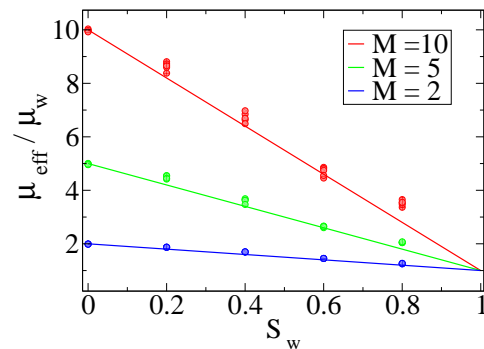


FIG. 4: The effective viscosity obtained from lattice Boltzmann simulations (dots) and compared with fits to equation (14) with  $\alpha = 1$ .

### Acknowledgments

The authors thank Dick Bedeaux, Carl Fredrik Berg, Signe Kjelstrup, Knut Jørgen Måløy, Per Arne Slotte and Ole Torsæter for interesting discussions. EGF and AH thank the Beijing Computational Science Research Center CSRC and Hai-Qing Lin for hospitality. SS was supported by the National Natural Science Foundation of China under grant number 11750110430. This work was partly supported by the Research Council of Norway through its Centers of Excellence funding scheme, project number 262644.

- 
- [1] J. Bear, *Dynamics of fluids in porous media* (Dover, Mineola, 1988).
- [2] K. T. Tallakstad, H. A. Knudsen, T. Ramstad, G. Løvoll, K. J. Måløy, R. Toussaint, and E. G. Flekkøy, *Phys. Rev. Lett.* **102**, 074502 (2009).
- [3] O. Aursjø, M. Erpelding, K. T. Tallakstad, E. G. Flekkøy, A. Hansen and K. J. Måløy, *Front. Phys.* **2**, 63 (2014).
- [4] R. D. Wyckoff and H. G. Botset, *J. Appl. Phys.* **7**, 325 (1936).
- [5] M. C. Leverett, *Trans. AIMME*, **12**, 152 (1940).
- [6] R. H. Brooks and A. T. Corey, Hydraulic properties of porous media, Hydrology Papers No. 3 (Colorado State Univ., Fort Collins, 1964).
- [7] L. W. Lake, *Enhanced oil recovery* (Prentice Hall, Englewood Cliffs, 1989).
- [8] W. H. McAdams, W. K. Woods and L. C. Heromans, *Trans. ASME*, **64**, 193 (1942).
- [9] A. Cicchitti, C. Lombardi, M. Silvestri, G. Soldaini and R. Zavattarlli, *Energia Nucleare*, **7**, 407 (1960).
- [10] M. M. Awad and Y. S. Muzychka, *Exp. Thermal and Fluid Sci.*, **33**, 106 (2008).
- [11] S. Sinha, A. Hansen, D. Bedeaux and S. Kjelstrup, *Phys. Rev. E*, **87**, 025001 (2013).
- [12] J. P. Straley, *Phys. Rev. B*, **15**, 5733 (1977).
- [13] K. Lichtenecker and K. Rother, *Phys. Z.* **32**, 255 (1931).
- [14] Y. Guéguen and V. Palciauskas, *Introduction to the physics of rocks* (Princeton Univ. Press, Princeton, 1994).
- [15] M. G. Todd and F. G. Shi, *IEEE Trans. Diel. and El. Insulation*, **12**, 601 (2005).
- [16] A. Brovelli and C. Cassiani, *Geophys. J. Int.* **180**, 225 (2010).
- [17] S. Kirkpatrick, *Rev. Mod. Phys.* **45**, 574 (1973).
- [18] E. Aker, K. J. Måløy, A. Hansen and G. G. Batrouni, *Transp. Porous Media*, **32**, 163 (1998).
- [19] C. P. Ody, C. N. Baroud and E. de Langre, *J. Colloid Interface Sci.* **308**, 231 (2007).
- [20] X. Liu, C. Zhang, W. Yu, Z. Deng and Y. Chen, *Sci. Bull.* **61**, 811 (2016).
- [21] S. Sinha, A. T. Bender, M. Danczyk, K. Keepseagle, C. A. Prather, J. M. Bray, L. W. Thrane, J. D. Seymour, S. L. Codd and A. Hansen, *Transp. Por. Med.* **119**, 77 (2017).
- [22] W. E. Langlois, *Slow Viscous Flow*, (The Macmillan Company, New York, 1964).
- [23] P. Jia, M. Dong, L. Dai and J. Yao, *Slow viscous flow through arbitrary triangular tubes and its application in modelling porous media flows*, *Transp. Porous Media* **74**, 153 (2008).
- [24] A. K. Gunstensen, D. H. Rothman, S. Zaleski and G. Zanetti, *Phys. Rev. A*, **43**, 4320 (1991).